XLVI CILAMCE
VITÓRIA - ES - BRAZIL - 2025
XLVI IBERO-LATIN AMERICAN CONGRESS ON COMPUTATIONAL METHODS IN ENGINEERING

A Modified FOSM Method for the Reliability Assessment of Cold-Formed Steel Members

André L. R. Brandão[1], Eloá F. Brandão[2], Giovanne de L. Santana[1], Marcílio S. R. Freitas[3]

[1]*Institute of Integrated Engineering, Federal University of Itajubá*
Itabira, 37.500-903, Minas Gerais, Brazil
andreriqueira@unifei.edu.br, *d2021006903@unifei.edu.br*
[2]*Civil Engineering Program, Federal University of Minas Gerais*
Avenida Antonio Carlos, 6627, 31270-901, Belo Horizonte/MG, Brazil
eloafbrandao@ufmg.br ,
[3]*Civil Engineering Program, Federal University of Ouro Preto*
Ouro Preto, 35.400-000, Minas Gerais, Brazil
marcilio@ufop.edu.br,

Abstract. The FOSM (First Order Second Moment) method is a structural reliability analysis technique that estimates the probability of failure based on the first two statistical moments (mean and variance) of the variables involved. Structural reliability assessments are often conducted using the FOSM method due to its simplicity and the absence of advanced computational requirements. Unlike more complex approaches—such as the First Order Reliability Method (FORM), which involves variable transformations and iterative procedures, or Monte Carlo Simulation (MCS), whose accuracy depends on a large number of simulations - FOSM provides a straightforward and practical framework, suitable for the calibration of design codes. However, this simplification compromises the accuracy of FOSM. This paper proposes a modified version of the FOSM method (denoted $FOSM_m$), which incorporates adjustment functions to better approximate the results of MCS in the reliability analysis of cold-formed steel members. The $FOSM_m$ method showed excellent agreement with MCS results for load combinations of the type D_n (nominal dead load) + L_n (nominal live load), with L_n/D_n ratios ranging from 0 to 10. Moreover, $FOSM_m$ proved to be effective when applied to typical ranges of load factors used in the design of structural members. The proposed methodology retains the simplicity of FOSM while significantly improving its accuracy, offering a robust and accessible alternative for structural reliability assessments.

Keywords: reliability, FOSM, FORM, MCS, Cold-Formed Steel.

1 Introduction

Structural reliability analysis has become an essential tool in the development and calibration of design codes, especially in the context of designing structural members under uncertainty. Among the various available methods, the FOSM (First Order Second Moment) method stands out for its simple and straightforward formulation, based only on the first two statistical moments of the random variables: the mean and the variance. This simplicity makes FOSM particularly attractive for practical applications, such as the calibration of partial safety factors, without the need for complex transformations or significant computational effort.

In several research studies (Tab. 1), the FOSM (First-Order Second-Moment) method has been widely used for the calibration of resistance factors in cold-formed steel (CFS) sections, following the recommendations of Chapter K, item K2.1.1 of the ANSI/SDI AISI S100 standard [1]. These studies include various approaches, such as numerical and experimental analyses on different cross-sections like channel, zee, sigma, tubular, racks, and built-up members. The research investigates innovative analytical methods for CFS design, examines the effects of holes in the web, explores interactions between buckling modes, and evaluates bolted and welded connections.

Table 1. Articles addressing calibration following item K2.1.1 of the ANSI/SDI AISI S100 standard [1]

Article Title	Year	Ref.
Effective section method: A general direct method for the design of steel cold-formed members under local-global buckling interaction.	2010	[2]
Resistance factor calibration for cold-formed steel compression members.	2013	[3]
Tests of cold-formed high strength steel tubular sections undergoing web crippling.	2017	[4]
Reliability analysis of welded and bolted connections in cold-formed steel sections.	2018	[5]
Resistance factor calibration for perforated cold-formed steel compression members.	2022	[6]
Reliability of cold-formed steel sections subjected to web crippling.	2023	[7]
Design of Cold-Formed Z-Shaped purlin-to-rafter connections subject to pull-through failure.	2024	[8]
Design of concrete-filled high-strength steel RHS and SHS tubes under bending.	2024	[9]
Cold-formed steel strength predictions for torsion and bending–torsion interaction.	2024	[10]
Influence of web holes on cold-formed steel beams: Experimental and numerical analysis.	2025	[11]
Design of short-to-intermediate slender built-up flanged cruciform columns.	2025	[12]
Structural reliability of the design of pallet-rack columns via Direct Strength Method.	2025	[13]
Lipped channel cold-formed steel columns: “all-in-one” design approach including the buckling interaction models LG, LD, DG and LDG.	2025	[14]

The simplification of the FOSM method, however, imposes important limitations, particularly regarding the accuracy of reliability estimates, especially in cases involving non-normal distributions, nonlinear performance functions, or multiple interdependent variables. More advanced methods, such as the FORM (First Order Reliability Method), SORM (Second Order Reliability Method), and MCS (Monte Carlo Simulation), offer greater theoretical rigor and precision but require iterative procedures and higher computational capacity, which are not always feasible in preliminary studies or in code calibration applications (Haldar and Mahadevan [15]).

This study aims to develop and evaluate a modified version of the FOSM method, referred to as $FOSM_m$, applied to the structural reliability analysis of cold-formed steel members. The main goals are to: (i) preserve the simplicity and low computational demand of the traditional FOSM method; (ii) incorporate adjustment functions that correct the typical inaccuracy of the method; (iii) verify the agreement between $FOSM_m$ results and Monte Carlo Simulation (MCS); (iv) assess the method's performance over a wide range of load ratios $\rho = L_n/D_n$; and (v) contribute to the calibration of technical design standards.

2 Reliability Methods

2.1 FOSM Method

Currently, the relative reliability of structural design rules, including the design equations for CFS members, is expressed in terms of a reliability index, commonly denoted as β. A higher value of β indicates greater reliability. A widely used method to compute the reliability index β is the FOSM (First Order Second Moment method) (Cornell [16]; Ellingwood et al. [17]; Hsiao [18]). Using this index, the target reliability values β_0 for cold-formed steel members are typically 2.5 for Load and Resistance Factor Design (LRFD) and 3.0 for Limit States Design (LSD), while for connections, the corresponding target values are higher, at 3.5 for LRFD and 4.0 for LSD [1]. The method assumes lognormal distributions for both the resistance R and the load Q, so that β is computed from:

$$\beta = \frac{ln\left(\frac{\mu_R}{\mu_Q}\right)}{\sqrt{\delta_R^2+\delta_Q^2}}. \tag{1}$$

where:
μ_R = mean of the resistance;
μ_Q = mean of the load;
δ_R = coefficient of variation of the resistance;
δ_Q = coefficient of variation of the load.

Since the resistance variable R can be expressed in terms of dimensionless variables normalized with respect to nominal values, namely M (material factor), F (fabrication factor), and P (professional factor), and the load variable Q can be expressed in terms of D (dead load) and L (live load), the reliability index can be calculated using eq. (2):

$$\beta_{FOSM} = \frac{ln\left(\left(\frac{1}{\phi}\right)\left(\frac{\gamma_D+\rho\gamma_L}{\mu_D+\rho\mu_L}\right)(\mu_M\mu_F\mu_P)\right)}{\sqrt{\delta_M^2+\delta_F^2+\delta_P^2+\left(\frac{\sqrt{(\mu_D\delta_D)^2+(\rho\delta_L)^2}}{(\mu_D+\rho\mu_L)}\right)^2}}. \tag{2}$$

where:
μ_D = normalized mean of dead load;
μ_L = mean of live load;
μ_M = mean of the material factor;
μ_F = mean of the fabrication factor;
μ_P = mean of the professional factor;
δ_M = coefficient of variation of the material factor;
δ_F = coefficient of variation of the fabrication factor;
δ_P = coefficient of variation of the professional factor;
δ_D = coefficient of variation of the dead load;
δ_L = coefficient of variation of the live load;
ϕ = resistance factor;
$\rho = L_n/D_n$ (nominal live-to-dead load ratio);
γ_D = load factor for dead load;
γ_L = load factor for live load.

From eq. (2), the following formula is derived for calibrating the resistance factor ϕ:

$$\phi = \left(\frac{\gamma_D+\rho\gamma_L}{\mu_D+\rho\mu_L}\right)(\mu_M\mu_F\mu_P)e^{-\beta_o\sqrt{\delta_M^2+\delta_F^2+\delta_P^2+\left(\frac{\sqrt{\left(\frac{\mu_D}{\rho}\delta_D\right)^2+(\mu_L\delta_L)^2}}{\left(\frac{\mu_D}{\rho}+\mu_L\right)}\right)^2}}. \tag{3}$$

Essentially, eq. (3) is the same as the equation provided in Chapter K, item K2.1.1 of the [1], i.e., eq. (4), which is also adopted in the Brazilian standard NBR 14762 [19].

$$\phi = C_\phi(\mu_M\mu_F\mu_P)e^{-\beta_o\sqrt{\delta_M^2+\delta_F^2+\delta_P^2+\delta_Q^2}}. \tag{4}$$

where:
C_ϕ = calibration coefficient;
δ_Q = coefficient of variation of the load effect;
β_o = target reliability index.

Table 2 presents the statistical data of the variables normalized with respect to their nominal values, M and F, as provided in Chapter K of the [1].

Table 2. Mean (μ) and coefficient of variation (δ) for normalized variables associated with material and fabrication variability

Type of Component	μ_M	δ_M	μ_F	δ_F
Members in Tension, Compression, Flexure, Shear or Web Crippling.	1.10	0.10	1.00	0.05
Members under Combined Forces	1.05	0.10	1.00	0.05
Welded Connections	1.10	0.10	1.00	0.05
Bolted Connections	1.10	0.08	1.00	0.05
Screw Connections	1.10	0.10	1.00	0.05

According to [17], the statistical characteristics of the normalized load variables are as follows: the mean and coefficient of variation for dead load are $\mu_D = 1.05$ and $\delta_D = 0.10$, respectively; while for live load, the mean is $\mu_L = 1.00$ and the coefficient of variation is $\delta_L = 0.25$.

2.2 Monte Carlo Simulation

Monte Carlo Simulation (MCS) is a numerical technique widely used to estimate the probability of failure of structures considering uncertainties in material properties, geometry, and applied loads. This method is especially useful when the limit state function is complex, nonlinear, or difficult to express analytically.

The formulation of the failure function in MCS starts with the basic limit state function G(.) = R - Q, where R and Q are random variables representing resistance and load effects, respectively. By expressing the failure function in terms of the variables M, F, P, D, and L, the function can be written as:

$$G(.) = R_n \boldsymbol{MFP} - (D_n \boldsymbol{D} + L_n \boldsymbol{L}). \tag{5}$$

Failure is defined by the condition $G(\cdot) \leq 0$, meaning that the structural resistance is less than or equal to the total applied load effect.

The MCS procedure involves several key steps: first, defining the probability distributions of all random variables M, F, P, D, and L; next, generating a large number N of random samples for these variables; then, calculating the limit state function value G_i for each set of samples, where the subscript *i* denotes the i-th sample or realization, with *i* ranging from 1 to N; subsequently, counting the number of failure occurrences where $G_i \leq 0$; and finally, estimating the probability of failure as the ratio between the number of failures N_f and the total number of samples N [15].

Ellingwood et al. [17] specify lognormal probability density functions (PDFs) for the variables M and F, a normal distribution for D, and a Gumbel distribution for L. The statistics for the professional factor P at each limit state are derived from a statistical analysis of a data set based on the ratio between experimental ultimate strength and theoretical (nominal) strength.

2.3 Modified FOSM Method

For the development of the modified FOSM method, curves of the reliability index β versus the nominal live-to-dead load ratio ρ were plotted using eq. (2) for a specific scenario with the following data: resistance factor ϕ = 0.91 (equivalent to a load factor γ of 1.10 [19]); mean and coefficient of variation for the professional factor, μ_P = 1.10 and δ_P = 0.10, respectively; load factors γ_D = 1.25 and γ_L = 1.5; and other statistical data related to members (Tab. 2). Subsequently, points (ρ, β) were calculated using MCS for the same scenario, incorporating the probability density functions (PDFs) as previously defined, and a lognormal PDF for the variable P. Figure 1a illustrates the FOSM curve as a blue dashed line and the MCS results as black triangle markers (▲▲▲▲). It is observed that the MCS points initially do not align well with the β_{FOSM} curve (eq. (2)).

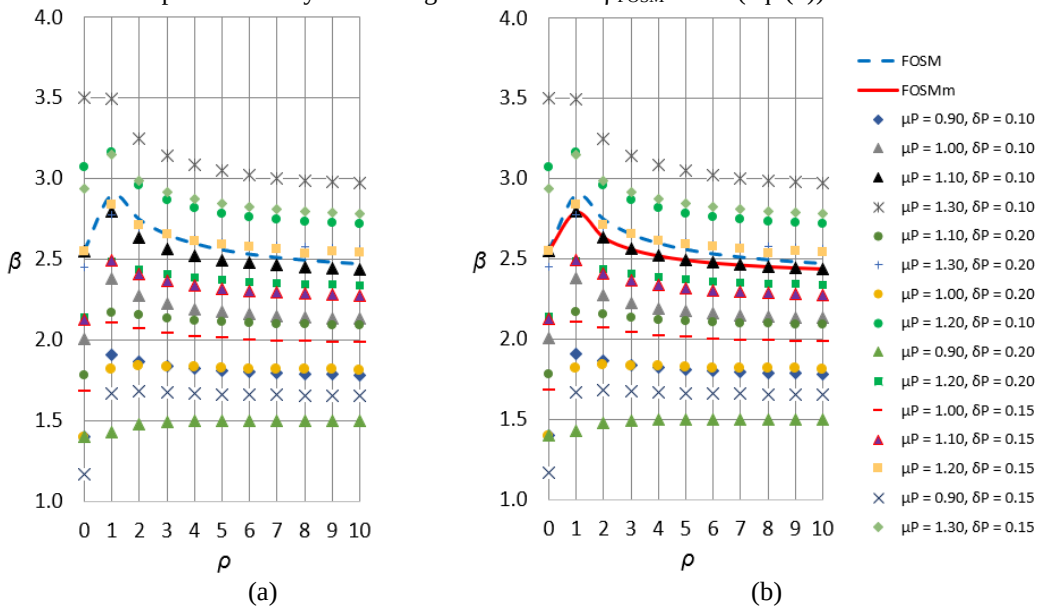


Figure 1. Reliability index: (a) β_{FOSM} curve with MCS results. (b) β_{FOSMm} curve fitted to the case defined by statistical parameters μP = 1.10 and δP = 0.10.

A detailed analysis demonstrated that by introducing specific constants A, B, C, and D into eq. (2), the resulting curve could be calibrated to closely match the MCS points. Consequently, the modified FOSM method (β_{FOSMm}) was established through the incorporation of these constants, as expressed in eq. (6).

$$\beta_{FOSMm} = \frac{ln\left(\left(\frac{1}{\phi}\right)\left(\frac{\gamma_D + A\rho\gamma_L}{\mu_D + A\rho\mu_L}\right)(\mu_M\mu_F\mu_P)\right)}{D\sqrt{\delta_M^2+\delta_F^2+C^2\delta_P^2+\left(\frac{\sqrt{(\mu_D\delta_D)^2+\left(A\rho^B\delta_L{}^B\right)^2}}{(\mu_D+A\rho\mu_L)}\right)^2}}. \tag{6}$$

When unit values are assigned to the constants A, B, C, and D, the curves β_{FOSM} (blue dashed line) and β_{FOSMm} (solid red line) are identical, indicating that no modification has been applied. For the scenario under study, satisfactory convergence was achieved by setting A=1.60, B=1.00, C=1.00, and D=1.00. With these values, the β_{FOSMm} curve closely matches the MCS points (▲▲▲▲), as shown in Fig. 1b.

To extend the applicability of the β_{FOSMm} formulation (eq. (6)), the other cases were also analyzed to obtain the constants A, B, and C. Table 3 presents the results for the remaining cases shown in Fig. 1.

Table 3. Scenarios (μ_P, δ_P) for the determination of constants A, B, and C.

μ_P	δ_P	A	B	C	μ_P	δ_P	A	B	C	μ_P	δ_P	A	B	C
1.30	0.10	1.80	1.01	1.11	1.20	0.20	1.40	1.00	1.01	0.90	0.20	0.66	0.96	0.96
1.30	0.15	1.12	0.99	1.10	1.00	0.10	1.60	0.99	0.99	1.20	0.15	1.19	0.99	1.06
1.20	0.10	1.60	1.00	1.09	1.00	0.15	1.10	0.98	0.99	1.10	0.15	1.14	0.99	1.03
1.30	0.20	1.44	1.00	1.07	1.10	0.20	1.08	0.98	0.97	1.00	0.20	0.85	0.98	0.97
1.10	0.10	1.60*	1.00*	1.00*	0.90	0.15	0.90	0.97	0.95	0.90	0.10	1.50	0.98	0.77

Note: * A, B, and C from the first studied scenario.

The results presented in Tab. 3 allowed the development of mathematical expressions for the parameters A, B, and C. To this end, multiple regression analysis was performed using μ_P and δ_P as independent variables, and A, B, and C as dependent variables. Polynomial models, including interaction and quadratic terms (e.g., μ_P^2, $\mu_P\delta_P$, etc.), were tested to improve the quality of fit.

Third-degree polynomial regressions provided the best results, with coefficients of determination of R^2 = 0.686 for A, R^2 = 0.767 for B, and R^2 = 0.981 for C. These values demonstrate that the models effectively capture the data trends, particularly for parameter C, where the predictive accuracy is excellent.

Equations (7), (8), and (9) present the resulting functions for parameters A, B, and C, respectively.

$$A = -22.1587 + 76.0899\mu_P - 76.0353\delta_P - 75.0873\mu_P^2 + 118.1493\mu_P\delta_P - 113.3109\delta_P^2 + 25.4873\mu_P^3 - 81.4588\mu_P^2\delta_P + 240.2456\mu_P\delta_P^2 - 46.0476\delta_P^3 \tag{7}$$

$$B = 1.3086 - 1.2338\mu_P + 1.6433\delta_P + 1.5193\mu_P^2 - 4.1743\mu_P\delta_P + 1.4630\delta_P^2 - 0.5354\mu_P^3 + 1.4717\mu_P^2\delta_P + 1.9273\mu_P\delta_P^2 + 0.5515\delta_P^3 \tag{8}$$

$$C = -6.6931 + 12.0402\mu_P + 45.2226\delta_P - 5.6831\mu_P^2 - 54.8832\mu_P\delta_P - 57.6493\delta_P^2 + 0.8360\mu_P^3 + 14.7795\mu_P^2\delta_P + 49.9905\mu_P\delta_P^2 - 28.8817\delta_P^3 \tag{9}$$

Figure 2 shows the fitted surfaces of third-degree polynomial models describing the parameters A, B, and C as functions of μ_P and δ_P. The models were generated via multiple polynomial regression using Python [20], allowing both accurate data fitting and clear visualization of each parameter's behavior.

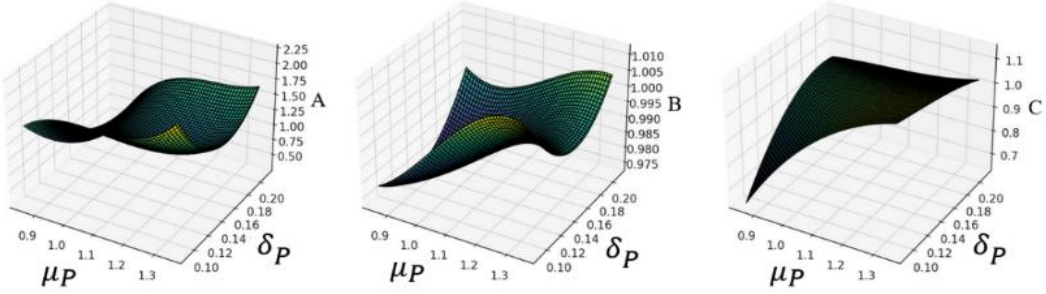


Figure 2. Graphs of the functions A, B, and C.

Finally, parameter D was defined by the function in eq. (10), covering resistance factor ϕ values from 0.50 to 0.99:

$$D = -0.2154\phi + 1.1958. \tag{10}$$

3 Method Validation and Application

Figure 3 illustrates reliability analysis results for typical design code scenarios, employing load statistics from [17] alongside other statistical data from Tab. 2. The specific parameters for each scenario are as follows: Scenario (a): $\mu_P = 0.90$, $\delta_P = 0.10$, load factor $\gamma = 1.10$, and load combination prescribed by [19] for simple bending; Scenario (b): $\mu_P = 1.10$, $\delta_P = 0.10$, resistance factor $\phi = 0.90$, and load combination according to LRFD [1] for simple bending; Scenario (c): $\mu_P = 1.12$, $\delta_P = 0.15$, resistance factor $\phi = 0.50$, and load combination specified by LSD [1] for bolted connections.

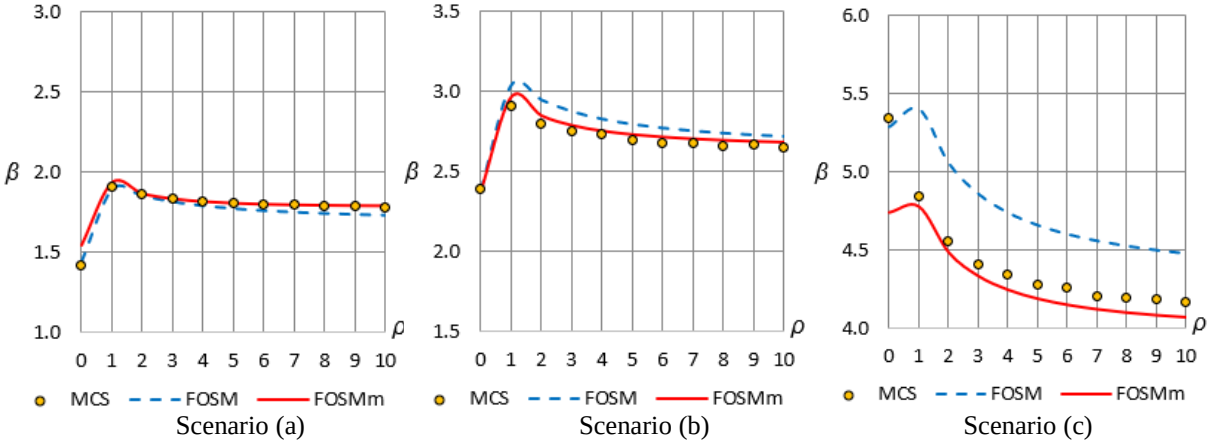


Figure 3. Reliability analysis results for typical design code scenarios.

In addition to varying β for ρ ranging from a value close to zero up to 10, different scenarios were analyzed to demonstrate the proposed method's applicability for various load combinations and ϕ values from 0.50 to 0.90. Good agreement was observed between the β_{FOSMm} and β_{MCS} curves. The relative errors of the reliability indices, calculated using eq. (11), are summarized in Tab. 3:

$$\varepsilon(\%) = \frac{|\beta_{Analytical} - \beta_{MCS}|}{|\beta_{MCS}|} \times 100 \tag{11}$$

where ε_F and ε_{Fm} represent the errors of the FOSM and FOSM$_m$ methods, respectively.

Table 3. Erro relativo (%).

	ρ	0	1	2	3	4	5	6	7	8	9	10
Scenario (a)	ε_F	1.58	0.59	0.58	1.08	1.54	1.91	2.18	2.40	2.55	2.68	2.80
	ε_{Fm}	8.57	1.55	0.09	0.17	0.20	0.17	0.08	0.02	0.14	0.27	0.37
Scenario (b)	ε_F	0.20	4.43	5.22	4.52	3.55	3.50	3.39	2.72	2.97	2.17	2.59
	ε_{Fm}	0.48	1.97	1.80	1.46	0.92	1.21	1.38	0.96	1.39	0.76	1.31
Scenario (c)	ε_F	0.91	11.71	10.94	10.23	9.22	8.86	8.02	8.29	7.75	7.38	7.37
	ε_{Fm}	11.20	1.25	1.59	1.68	2.13	2.08	2.54	2.06	2.33	2.50	2.34

Table 3 shows that the relative error ε_{Fm} for β_{FOSMm} was much lower than ε_F, except at very low ρ values. The FOSM$_m$ method significantly improves the accuracy of the reliability index β compared to the traditional FOSM. Although scenario (c) with $\phi = 0.50$ had higher ε_{Fm}, the improvement over the traditional method justifies using the modified approach.

4 Conclusions

The modified FOSM method ($FOSM_m$), through the integration of carefully calibrated adjustment functions, has demonstrated excellent agreement with Monte Carlo Simulation (MCS) results while preserving the computational efficiency inherent to the original FOSM approach. This balance of accuracy and simplicity positions $FOSM_m$ as a robust and practical tool for structural reliability assessments, especially suited for the calibration of design standards and preliminary reliability evaluations of cold-formed steel members. The method has proven effective for resistance factors (ϕ) ranging from 0.50 to 0.99, typical load factors (γ_D, γ_L) found in major cold-formed steel design codes, and a wide range of statistical variations in resistance and load parameters.

Acknowledgements. The authors gratefully acknowledge the support of UNIFEI, UFMG, UFOP, CNPq and FAPEMIG.

Authorship statement. The authors hereby confirm that they are the sole liable persons responsible for the authorship of this work, and that all material that has been herein included as part of the present paper is either the property (and authorship) of the authors, or has the permission of the owners to be included here.

References

[1] ANSI/SDI AISI S100, "North American Specification for the Design of Cold-Formed Steel Structural Members", American Iron and Steel Institute, Washington, DC, 2024.
[2] E.M. Batista, "Effective section method: A general direct method for the design of steel cold-formed members under local-global buckling interaction". *Thin-Walled Structures*. v.48, issue 4-5, p. 345-356, 2010.
[3] M. S. R. Freitas, A. L. R. Brandão and A. M. S. Freitas, "Resistance factor calibration for cold-formed steel compression members". *REM: Revista Escola de Minas*, 66(2), 233–238, 2013
[4] H. T. Li and B. Young, "Tests of cold-formed high strength steel tubular sections undergoing web crippling". *Engineering Structures*, 141, 571–583. https://doi.org/10.1016/j.engstruct.2017.03.051, 2017.
[5] M. S. R. Freitas, A. L. R. Brandão and A. R. Alves, "Reliability analysis of welded and bolted connections in cold-formed steel sections". *REM - International Engineering Journal*, 71(3), https://doi.org/10.1590/0370-44672016710087, 2018.
[6] R. L. F. Jardim, M. S. R. Freitas and A. L. R. Brandão, "Resistance factor calibration for perforated cold-formed steel compression members". *Revista Ingeniería de Construcción*, 37(1), 35–46. https://www.ricuc.cl, 2022.
[7] N. B. Melo, M. S. R. Freitas and A. L. R. Brandão, "Reliability of cold-formed steel sections subjected to web crippling". *Structural Engineering International*, 34(2), 196–202. https://doi.org/10.1080/10168664.2023.2249494, 2024.
[8] H. Karthikeyan, B. Naik and M. Madhavan, "Design of cold-formed Z-shaped purlin-to-rafter connections subject to pull-through failure". *Thin-Walled Structures*, 199, 111725. https://doi.org/10.1016/j.tws.2024.111725, 2024.
[9] Y.-Q. Deng, Y. Huang and B. Young, "Design of concrete-filled high-strength steel RHS and SHS tubes under bending". *Engineering Structures*, 320, 118891. https://doi.org/10.1016/j.engstruct.2024.118891, 2024.
[10] Y. Xia, R. S. Glauz, B. W. Schafer, M. Seek and H. B. Blum, "Cold-formed steel strength predictions for torsion and bending-torsion interaction". *Thin-Walled Structures*, 195, 111367. https://doi.org/10.1016/j.tws.2023.111367, 2024.
[11] R. Oruç, "Influence of web holes on cold-formed steel beams: Experimental and numerical analysis". *Structures*, 74, 108471. https://doi.org/10.1016/j.istruc.2025.108471, 2025.
[12] J. Dobrić, N. Gluhović, A. Filipović, M. Samardžić-Petrović, X. Ruan and B. Rossi, "Design of short-to-intermediate slender built-up flanged cruciform columns". *Thin-Walled Structures*, 212, 113181. https://doi.org/10.1016/j.tws.2025.113181, 2025.
[13] V. A. M. Faria, M. S. R. Freitas and A. L. R. Brandão, "Structural reliability of the design of pallet-rack columns via Direct Strength Method". *Thin-Walled Structures*, 213, 113294. https://doi.org/10.1016/j.tws.2025.113294, 2025.
[14] E. M. Batista, G. Y. Matsubara, M. S. R. Freitas, V. A. M. Faria and A. L. R. Brandão, "Lipped Channel cold-formed steel columns: "all-in-one" design approach including the buckling interaction models LG, LD, DG and LDG". *Proceedings of the Annual Stability Conference, Structural Stability Research Council, Louisville, Kentucky*, 2025.
[15] A. Haldar and S. Mahadevan. *Probability, Reliability and Statistical Methods in Engineering Design*. John Wiley & Sons, New York, NY, 2000.
[16] A. C. Cornell, "A probability-based structural code". *ACI Journal*, v.66, 12, p.974-985, 1969.
[17] B. Ellingwood, T. V. Galambos, J. G. MacGregor, and C. A. Cornell, "Development of a probability-based load criterion for American National Standard A58: Building code requirements for minimum design loads in buildings and other structures". *National Bureau of Standards*, U.S. Department of Commerce, 1980.
[18] L.E. Hsiao. Reliability Based Criteria for Cold-Formed Steel Members. PhD Thesis, University of Missouri-Rolla, 1989.
[19] ABNT, NBR 14762, "Design of Cold-Formed Steel structures" (in Portuguese), ABNT, Rio de Janeiro, Brazil, 2010.
[20] Python Software Foundation. Python (Version 3.11) [Computer software]. https://www.python.org/, 2023.